

Final Draft
of the original manuscript:

Chen, Y.; Yang, X.; Zhao, L.; Almasry, L.; Haramus, V.M.;
Willumeit, R.; Zou, A.:

**Preparation and characterization of a nanostructured lipid
carrier for a poorly soluble drug**

In: *Colloids and Surfaces A* (2014) Elsevier

DOI: [10.1016/j.colsurfa.2014.04.032](https://doi.org/10.1016/j.colsurfa.2014.04.032)

Preparation and Characterization of a nanostructured lipid carrier for a poorly soluble drug

Yiyin Chen^{a#} Xiaomin Yang^{a#} Lin Zhao^c László Almásy^d Vasil M. Garamus^b Regine Willumeit^b Aihua Zou^a

^aState Key Laboratory of Bioreactor Engineering and Institute of Applied Chemistry, East China University of Science and Technology, Shanghai 200237, PR China,

^bHelmholtz-Zentrum Geesthacht: Centre for Materials and Coast Research, Institute of Materials Research, Max-Planck-Str. 1, D-21502 Geesthacht, Germany

^cSchool of Radiation Medicine and Protection, Soochow University Medical College, Suzhou 215123, China

^dWigner Research Centre for Physics, Institute for Solid State Physics and Optics, Budapest 1525 POB 49,
Hungary

* To whom correspondence should be addressed. Tel/Fax.: +86-21-64252231

E-mail: aihuazou@ecust.edu.cn.

^aEast China University of Science and Technology.

^bHelmholtz-Zentrum Geesthacht.

^cSoochow University Medical College

^dWigner Research Centre for Physics

[#]These authors contributed equally to this work

Abstract:

The aim of this study was to prepare a stable nanostructured lipid carrier (NLC) with biocompatible lipids and surfactants (Pluronic F68 and Cremophor EL) by high-pressure homogenization (HPH). Surface tension measurements were used to choose the suitable ratio between Pluronic F68 and Cremophor EL. Hydrophobic anticancer drug docetaxel (DTX) was used as active pharmaceutical ingredient (API). The mean particle size of docetaxel loaded nanostructured lipid carrier (DTX-NLC), as determined by dynamic light scattering (DLS), was between 120 nm to 250 nm during the storage period of 30 days, with the entrapment efficiency decreasing from $(60.5 \pm 5.0)\%$ to $(55.3 \pm 4.5)\%$, while zeta potential was slightly changed from (-43.19 ± 3.6) mV to (-40.12 ± 4.3) mV. Transmission electron microscopy (TEM) showed that some of DTX-NLCs have elongated shape. Small angle neutron scattering (SANS) demonstrated that DTX-NLC in solution contained dense core with perfectly smooth surface, while blank NLC had dense core but rough surface. The blank NLC and DTX-NLC showed cubic crystalline structure according to small angle X-ray scattering (SAXS). Wide angle X-ray diffraction (XRD) showed that adding of DTX increased the crystallinity of the NLC. Cytotoxicity was studied by MTT assay against HeLa cells. The data suggested that blank NLC was biocompatible with HeLa cells while the DTX-NLC was more cytotoxic than pure DTX at the same drug concentration. DTX-NLC could be taken up into the cells more than pure DTX, which could be attributed to the better solubility of DTX after loading into NLC.

Keywords Nanostructured lipid carrier; docetaxel; SANS; SAXS; cytotoxicity

1. Introduction

Drug delivery device is reported to enhance efficiency and reduce side effects of cytotoxic drugs. Various advanced nanostructures (including micelles, liposomes, solid lipid nanoparticles, nanostructured lipid carriers and polymeric nanoparticles) have been developed. ^[1] The lipid nanoparticles (~~including solid lipid nanoparticles and nanostructured lipid carriers~~) are composed of lipids similar to physiological ones, ~~which offer~~ various advantages making them the ideal delivery vehicles. **Nanostructured Lipid Carrier (NLC)** is the second generation of lipid nanoparticles. Comparing with solid lipid nanoparticle (SLN), NLC is produced by controlled mixing of solid lipids with **spatially** incompatible liquid lipids, which **results in special nanostructures** with improved properties for drug loading and stable drug incorporation during storage. ^[2] Lipid nanoparticles have been proposed as alternative carriers to well-known liposomes and polymeric nanoparticles in order to overcome some of common problems. The application of lipid nanoparticles is very wide including cancer treatment, transfection, liver targeting, imaging, targeting the central nervous and etc. ^[3] Daniela M.R. ~~etc.~~ prepared tretinoin loaded Chitosan-solid lipid nanoparticles (SLNs-chitosan-TRE) for skin delivery. They found that SLNs-chitosan-TRE had high encapsulation efficiency, high physical stability for one year, were not cytotoxic to keratinocytes and had high antibacterial activity against *P. acnes* and *S. aureus*. ^[4]

Recently the shape and microstructure of carriers have been identified as one of key factors that influence important biological processes, including biodistribution

and cellular uptake. ^[5] Many investigations have led to significant advances in understanding the impact of key NLC properties such as size, surface chemistry and shape on their performance. ^[6-8] For better understanding of lipid nanoparticles and their controlled release development, it is necessary to study the inner microstructure of this special lipid matrix. ^[9] ~~In this study, small angle neutron scattering and small angle X-ray scattering were used to determine the microstructure of the lipid carrier~~

Docetaxel is reported as an inhibitor of microtubule depolymerization and has broad antitumor activities against a variety of solid tumors, including breast, non-small cell lung cancer, ovarian and so on. ^[10-13] However, its clinical efficiency is limited due to its poor solubility, low bioavailability and high toxicity. ^[14] Various drug carriers including hyaluronic acid-ceramide (HA-CE)-based self-assembled nanoparticles^[15], liposomal nanoparticles^[16] and solid lipid nanoparticles^[17] were used to load DTX to broaden its clinical application. ^[18-21] ~~Some researchers have prepared docetaxel-loaded SLN with a galactosylated conjugated DOPE lipid to specifically target the asialo-glycoprotein receptor on hepatocellular carcinoma cells. ^[22] Li etc. have prepared freeze-dried docetaxel NLCs, which had a spherical or ellipsoid shape, with 97.6% drug entrapment efficiency. They found that freeze-dried docetaxel NLCs showed high uptake in RES organs after intravenous administration, and the docetaxel concentration in the lungs was significantly higher with NLCs than following injection of docetaxel solution. ^[23] An improved cytotoxicity against A549 cells has also been obtained by encapsulating docetaxel in NLCs. The inhibition rate of docetaxel NLCs was 90.36%, while that of commercial Duopafei[®] was only 42.74%,~~

indicating that docetaxel NLCs are more effective inhibitors of tumor growth. [24]

In the present study, DLS, TEM, SANS, SAXS and XRD measurements were used for structure characterization including shape, size and inner microstructure of NLC, and DTX was used as API to study the effects of lipophilic drug on NLC.

2. Materials and methods

2.1 Materials

Docetaxel (DTX 99.5%, Shanghai JinHe Co. Ltd, China), stearic acid (SA, LingFeng Chemical Reagent Co. Ltd, China); glycerin monostearate (MGE, Aladdin Chemical Reagent Co. Ltd, China); oleic acid (OA, Aladdin Chemical Reagent Co. Ltd, China); capric/caprylic triglycerides (MCT, Aladdin Chemical Reagent Co. Ltd, China); Cremophor EL (EL, Aladdin Chemical Reagent Co. Ltd, China); Pluronic F68 (F68, Adamas Reagent Co. Ltd, China); freshly prepared double distilled and ultra purified water; trehalose (Aladdin Chemical Reagent Co. Ltd, China); 3-(4,5-dimethylthiazol-2-yl)-2,5-diphenyltetrazolium bromide (MTT, Sigma, China). D2O (Sigma, Germany). All other chemicals were of analytical grade.

2.2 Preparation of nanostructured lipid carrier

Blank NLC and DTX-NLC were prepared by HPH. In brief, aqueous and oil phase were prepared separately. Lipid mixtures (SA, MGE, MCT and OA) were maintained at 70 °C to prevent the recrystallization of lipids during the process, and then DTX was added to oil phase until it totally melted. The same temperature aqueous phase (F68, EL and ultra purified water) was added to the oil phase with intense stirring (10000 rmp for 1 min; Turrax T25, Fluko, Germany). The dispersion

was processed through a high-pressure homogenizer with five homogenization cycles at 600 bar. The nanodispersion was cooled overnight at room temperature. Appropriate amounts of Trehalose (3%, w/v) were used to dilute the NLCs dispersion. All the samples were frozen at -78 °C for 10h before being lyophilized for 36 h. The freeze-dried powders were rehydrated at phosphate buffer solution buffer (PBS, pH7.4) for later experiments.

2.3 Surface tension

The surface tension was measured by Wilhelmy small plate method on liquid measuring apparatus Dataphysics (DCAT21, Germany) at room temperature. The platinum plate was first cleaned and roasted in a red flame before each measurement. ~~The system was corrected by purified water, and~~ The data was calibrated to the surface tension of purified water. All the samples were measured three times.

2.4 Dynamic light scattering

The mean particle size and polydispersity index (PDI) of blank NLC and DTX-NLCs were measured three times by dynamic light scattering at 25 °C using Nano-ZS90 system (DLS, Malvern Instruments Ltd., UK) with a measurement angle of 90 °.

2.5 Entrapment efficiency and drug loading

Briefly, the desired amount of DTX-NLCs was rehydrated in PBS (pH 7.4) and ~~was centrifuged for 15 min at 12,000 rpm at 4 °C to remove the untrapped drug from samples. The upper aqueous phase from first step was placed into centrifuge tube and methanol was added to destroy the structure of NLCs. Then the suspension~~

was subjected to 15 min centrifugation at 12,000 rpm at 4 °C. The precipitate was the entrapped DTX. The contents of DTX were determined by high performance liquid chromatography (HPLC) (WuFeng Instruments Ltd, China) method: Diamond C18 column (150 mm × 4.6 mm i.d, pore size 5 µm, A yi te, China), the mobile phase CH₃CN: MeOH: H₂O = 30:40:30 (v/v/v), flow rate 1 ml/min, and wavelength 230 nm. The concentration of DTX against calibration curve of peak area was $C=0.00128A - 2.01492$ ($R^2 = 0.999$). All experiments were conducted at room temperature (25 °C). The drug loading (DL%) and entrapment efficiency (EE%) were calculated by following formulas:

$$DL\% = \text{weight of DTX encapsulated in NLC} / \text{weight of DTX-NLC} \times 100;$$

$$EE\% = \text{the calculated DL} / \text{the theoretical DL} \times 100.$$

2.6 Transmission Electron Microscopy

The ~~shape and~~ morphologies of NLCs were determined by JEM-1400 electron microscope (JEOL, Tokyo, Japan). For TEM measurement, samples were prepared by placing a drop of fresh prepared DTX-NLC and Blank-NLC suspension onto a copper grid and air-dried, followed by negative staining with a drop of 1% aqueous solution of sodium phosphotungstic acid for contrast enhancement. Then the samples were dried in the air before TEM observation. ^[25]

2.7 Small Angle Neutron Scattering (SANS)

SANS measurements were performed on the Yellow Submarine instrument at the BNC in Budapest (Hungary). ^[26] The overall q-range was from 0.03 to 1 nm⁻¹. The

samples were filled in Hellma quartz cells of 2 mm path length and placed in a thermostated holder kept at 20.0 ± 0.5 °C. The raw scattering patterns were corrected for sample transmission, room background, and sample cell scattering. The 2-dimensional scattering patterns were azimuthally averaged, converted to an absolute scale and corrected for detector efficiency dividing by the incoherent scattering spectra of 1 mm thick pure water. The scattering from PBS buffer prepared in D₂O was subtracted as the background.

2.8 Small Angle X-ray Scattering (SAXS)

The SAXS measurements were performed at a laboratory SAXS instrument (Nanostar, Bruker AXS GmbH, Karlsruhe, Germany). Instrument includes I μ S micro-focus X-ray source with power of 30 W (used wavelength Cu K α) and VÅNTEC-2000 detector (14x14 cm² and 2048x2048 pixels). Sample to detector distance is 108.3 cm and accessible q range from 0.1 to 2.3 nm⁻¹.

2.9 Wide Angle X-ray powder diffraction (XRD)

Crystalline structure of DTX, ~~unloaded~~ blank NLCs and DTX-NLCs were investigated by D/MAX 2550 VB/PC X-ray diffractometer (Rigaku, Japan) using a Cu K α radiation source. Aqueous blank NLC and DTX-NLC were lyophilized before the XRD measurement. Diffractograms were recorded from the initial angle $2\theta = 10^\circ$ to the final angle 60° . The obtained data were collected with a step width of 0.02° and a count time of 1s.

2.10 Cell culture

The human cervical cancer cell line HeLa was purchased from American Type

Culture Collection (Manassas, VA, USA). HeLa cells were seeded onto cell culture dishes containing DMEM and RPMI-1640 respectively supplemented with 10% fetal bovine serum, L-glutamine (5 mmol/L), non-essential amino acids (5 mmol/L), penicillin (100 U/ml), and streptomycin (100 U/ml) (Invitrogen, Carlsbad, CA, USA), at 37 °C in humidified 5% CO₂ atmosphere.

2.11 In vitro cellular cytotoxicity assays

Cell viability was measured by 3-(4,5-dimethylthiazol-2-yl)-2,5-diphenyltetrazoliumbromide (MTT) assay. Both HeLa cells and MDA-MB-231 cells were plated in 96-well plates with 100 µl DMEM and RPMI-1640 media containing 10% fetal bovine serum at a density of 8×10^3 per well. After 12 h, the media were replaced by the media which contain DTX and DTX-NLC at equivalent DTX concentration (12, 24, 60, 120 nM). Blank NLC without DTX was added at the same volume as DTX-NLC. After 24 h, 20 µl MTT solution (5 mg/ml) was added to the medium per well. Cells were incubated for an additional 4 h. Then, the medium was removed. 150 µl of DMSO was added to dissolve the crystals formed by living cells. The absorbance was measured using an enzyme-linked immunosorbent assay reader at 570 nm, with the absorbance at 630 nm as the background correction. The cell viability was expressed as the percentage of untreated controls.

3. Results and discussion

3.1 Preparation of nanostructured lipid carrier

The composition of nanoparticle shells significantly affects the in vitro release of medicine and its performance in blood. ^[27-28] It is important to choose suitable

surfactants for NLC preparations. In our study, the drug delivery system was stabilized with two non-ionic surfactants, Pluronic F68 and Cremophor EL. Cremophor EL is FDA approved, and already clinically used for intravenous injection. The long PEG tail of Pluronic F68 can also act as a steric stabilizer. Both of them are common for the preparations of SLN and NLC.

Surface tension was measured to determine the optimal ratio between F68 and EL and also their concentrations. Given the fact that the surface tension was changing in the first several hours after preparation, all experiments were performed 24 hours later. As revealed by Table 1, adding of EL as co-surfactant was helpful for higher emulsifying efficiency. For example, at 1mg/ml surfactant concentration, the surface tension dropped from 46.34 ± 0.20 mN/m to 42.07 ± 0.23 mN/m when the ratio between F68 and EL varied from 1/0 to 1/1 and stayed constant within experimental errors with further addition of EL. In fact, many polysorbate molecules such as Tween-80 and Crempher are highly hydrophobic; hence they are formulated as delivery ingredients in current preclinical studies. However, such surfactants can cause significant hypersensitivity and toxicity issues, especially if multiple doses are used, ^[29-31] so F68 is more advantageous. In addition, it was found (see Table 1) that the surface tension was decreasing with higher surfactant concentration, but it did not change much when the ratio between F68 and EL were 1/1 and 1/2. It was reported that too much surfactants would result in drug burst release and NLC instability. ^[32-33]

From Table 1, it can be seen that pure EL has lower surface tension than pure F68, especially at the concentration of 1mg/ml, which indicate that EL has better surface

activity than F68. So, the surface tension of F68/EL solution will decrease with the addition of EL to F68 solution. Therefore, the diminishing effect of F68/EL ratio on surface tension is more pronounced at higher mass concentration (10 mg/ml). Consequently, the ratio between F68 and EL was fixed as 1/1, and the concentration of surfactants was 5 mg/ml for the reason that 1mg/ml surfactants may result in poor long-term stability of NLC.

Table 1

The surface tension of F68/EL aqueous solution at different molar ratio and concentration. Values are mean \pm SD (n=3)

Surfactant	Surface tension(mN/m)		
	1 mg/ml	5 mg/ml	10 mg/ml
F68/EL=1/0	46.34 \pm 0.20	43.35 \pm 0.24	41.66 \pm 0.10
F68/EL=1/0.5	45.21 \pm 0.12	43.28 \pm 0.15	41.01 \pm 0.25
F68/EL=1/1	42.07 \pm 0.23	40.58 \pm 0.22	40.72 \pm 0.33
F68/EL=1/2	42.70 \pm 0.22	40.93 \pm 0.12	40.38 \pm 0.20
F68/EL=0/1	41.75 \pm 0.45	40.77 \pm 0.10	40.69 \pm 0.20

The liquid lipids were reported to promote the formation of small-particles as a result of the higher mobility of the matrix. [35-36] OA and MCT mixed with solid lipids (SA and MGE) were used as core materials for the NLC due to their good solubilization of the poorly soluble drug. The ratios between them also influence strongly the mean particle size and polydispersity index of DTX-NLC. In addition to

being lipid core, SA and MGE provide emulsification and form more rigid surfactant films.^[34] It is reported that the oil precipitates separately at high concentration during cooling process. The location of the separated oil phase depends on the nature of lipid components, the ratio between lipids and production conditions.^[37] Finally, the ratio between solid/liquid lipid was fixed as 2/1.^[18] MCT as a liquid lipid provides thermodynamic stability and high solubility for many drugs.^[38] The particle size of formulation $L_{\text{mix-1}}$, $L_{\text{mix-2}}$, $L_{\text{mix-3}}$ and $L_{\text{mix-4}}$ were (190.7±3.2) nm, (143.9±5.0) nm, (139.8±1.9) nm and (136.4±3.5) nm after one day of preparation. Formulation ($L_{\text{mix-2}}$ vs $L_{\text{mix-1}}$, and $L_{\text{mix-4}}$ vs $L_{\text{mix-3}}$) with high MCT had smaller size, while the incorporation of OA increased the particle size and the polydispersity index (PDI). This was because OA increased the mobility of the internal lipids and fluidity of the surfatant layer due to the low melting point of OA.^[39] Also the particle diameters of $L_{\text{mix-3}}$ and $L_{\text{mix-4}}$ were smaller than those of $L_{\text{mix-1}}$ and $L_{\text{mix-2}}$. Therefore, 1.5/1 and 2.5/1 was chosen as the ratio of MGE/SA and MCT/OA, respectively. As it can be seen from Fig. 1, all samples remained stable in the period (the mean diameter and polydispersity index did not exhibit obvious changes). The particle diameters of $L_{\text{mix-2}}$, $L_{\text{mix-3}}$ and $L_{\text{mix-4}}$ were (145.9±3.0) nm, (136.4±2.4) nm, (136.4±3.1) nm in 48 hours after preparation and (151.6±2.9) nm, (148.2±0.6) nm, (137.5±1.2) nm in 192 hours after preparation, respectively. Combining with the results of polydispersity index, $L_{\text{mix-4}}$ was chosen for further investigation.

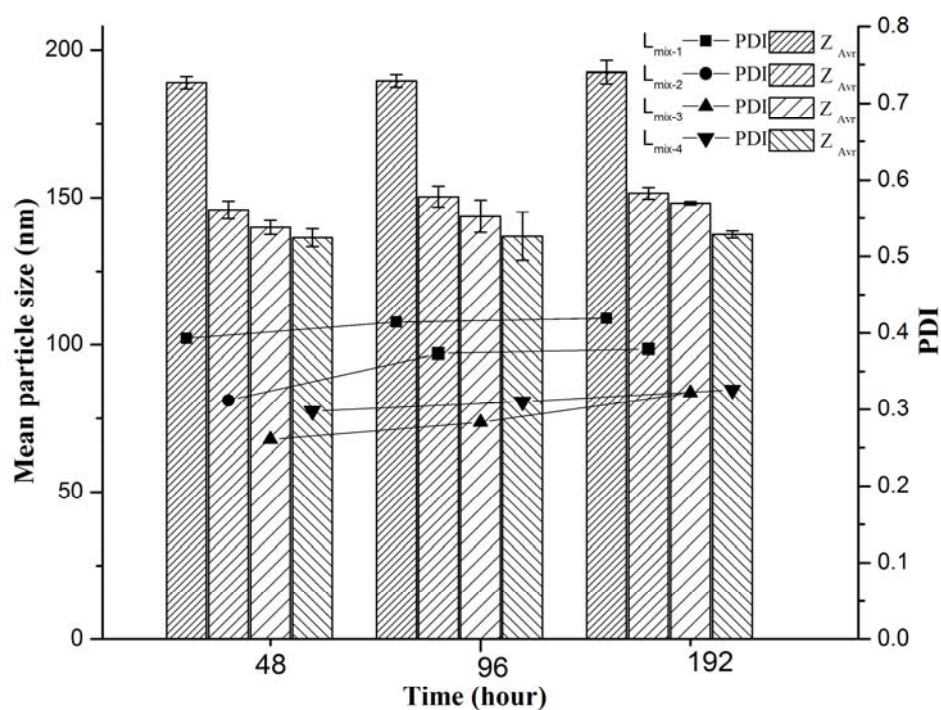
Table 2

The mass ratio between different lipids ingredients.

$L_{\text{mix-n}}$	*MGE /*SA (m/m)	*OA/*MCT (m/m)
$L_{\text{mix-1}}$	2/1	1/1
$L_{\text{mix-2}}$	2/1	1/2.5
$L_{\text{mix-3}}$	1.5/1	1/2
$L_{\text{mix-4}}$	1.5/1	1/2.5

*MGE is Monoglyceride; SA is Stearic acid; MCT is capric/caprylic triglycerides; OA is oleic acid.

Fig. 1. The mean particle size and PDI of NLC with different lipids ingredients in the storage of 8 days. Data are given as mean \pm SD (n=3)



The formulation composition was as follows: In 100 ml of ultra purified water, there were 596 mg SA, 1047 mg MGE, 593 mg MCT and 237 mg OA as oil phase. Then, 250 mg F68, 250 mg EL, and 5 mg of DTX as drug were added.

3.2 Entrapment efficiency and drug loading

As shown in Table 3, the mean particle size and PDI of both blank NLC and DTX-NLC increased a lot after 30 days of preparation, which indicated that some big

particles appeared. The enlarged lyophilised particle size may be explained by an increased hydrodynamic diameter of the NLCs due to coating of the particle surface with the saccharides through hydrogen bonding with lipids. [23] It is expected that the solid state of the lyophilisation will have a better chemical and physical stability than aqueous lipid dispersions. However, two additional transformations between the formulations might be the source of additional stability problems. The first transformation - from aqueous dispersion to powder - involves the freezing of the sample and the evaporation of water under vacuum. Freezing of the sample might cause stability problems due to the freezing out effect which results in changes of the osmolarity and the pH. The second transformation - resolubilization - involves, at least in its initial stages, situations which favor particle aggregation (low water and high particle content, high osmotic pressure). [40]

In addition, the encapsulation efficiency values of DTX-NLC decreased from (60.5±5.0) % to (55.3±4.5) %, and drug loading values also reduced from (0.28±0.01) % to (0.18±0.02) %, which meant some drug had been released from NLC. It was reported that during cooling process after HPH, some drug may locate in the surface layer instead of the core of NLC, and it was likely that these DTX were lost in the following days. [41] The surfactants and lipids can form micelles, liposomes and other aggregates in aqueous solution. DTX can also be loaded into these aggregates. So, there is no obvious drug separation found in samples after rehydration. But it was likely that these DTX easily lost during the re-dispersion process. The decrease of DL% is shown in Table 3. This phenomenon is similar with results reported by K. Zheng etc. [42] Other factors such as freezing and drying could also lead to DTX losses. It must be noticed, the load amount of DTX in sample was greatly decreased from 1 day to 30 days, which has been described as the drug burst release by Müller etc. for a number of SLN and it also could not be avoided for NLC. [40,43-45] To achieve prolonged release, special production conditions such as low surfactant content and low preparation temperature are recommended. [46] Moreover, the DL% and EE% of DTX-NLC were not as high as reported before. [20-21] The main reason was the limited solubility of DTX in the chosen lipid mixture. DTX is water-insoluble. According to

our experiments, the solubility of DTX in molten SA, MGE, MCT and OA were 5.2 mg/g, 17.7 mg/g, 7.9 mg/g and 18.9 mg/g, respectively. It is obvious that the solubility of DTX in these lipids was much higher compared to water. In a previous work, it was found that 1614 mg lipid mixture composed by SA, MGE, MCT and OA could dissolve 200mg CMT-3, which was a lipophilic drug too ^[47]. It was proved that these lipids can improve the solubility of water-insoluble drug. However, this improvement for DTX was still limited.

To assess system stability, zeta potential measurement was further performed. The zeta potential values of blank-NLC and DTX-NLC (in the first day preparation) of were (-49.99±4.7) mV and (-43.19±3.6) mV, respectively. After 30 days storage, the zeta potential was slightly changed to (-44.58±5.2) mV and (-40.12±4.3) mV, respectively. Thus, the zeta potential values of both blank-NLC and DTX-NLC could indicate that both samples seemed to be relatively stable after 30 days storage, although the obvious change of particle size, entrapment efficiency and drug loading.

Table 3

Physical characterization of blank NLC and DTX-NLC in day 1 and day 30 after preparation.

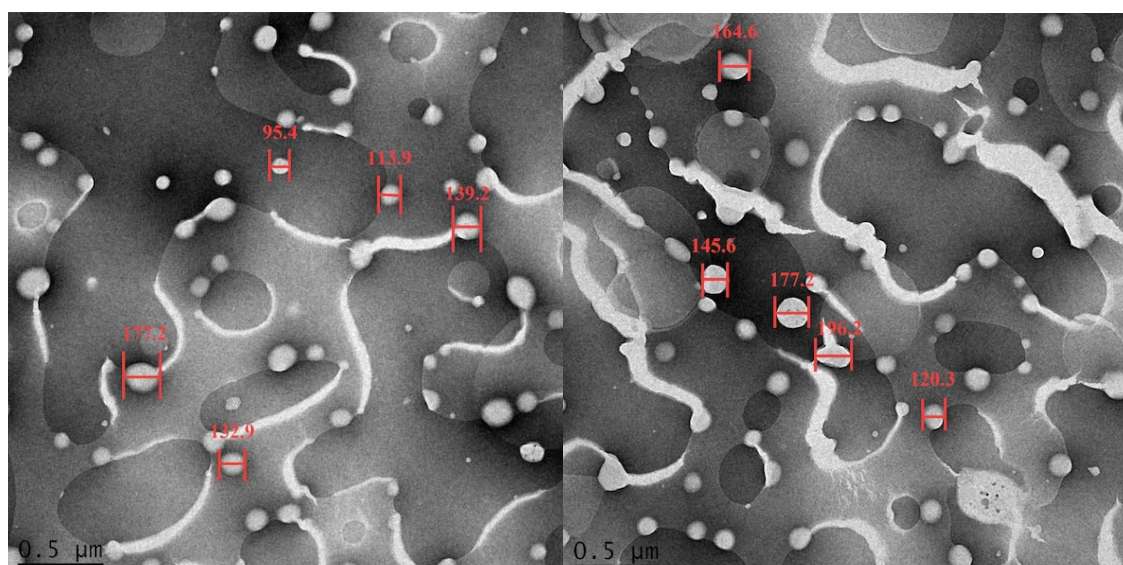
Formulations		1 day	30 days
DL%	Blank NLC	0	0
	DTX-NLC	0.28±0.01	0.18±0.02
EE%	Blank NLC	0	0
	DTX-NLC	60.0±5.0	55.3±4.5
Diameter (nm)	Blank NLC	136.4±3.5	169.3±0.5
	DTX-NLC	145.6±2.5	200.5±10.2
PDI	Blank NLC	0.29	0.42
	DTX-NLC	0.33	PDI
Zeta Potential (mV)	Blank NLC	-49.99±4.7	-44.58±5.2
	DTX-NLC	-43.19±3.6	-39.12±4.3

Note: PDI means polydispersity index. Data were given as mean ± SD (n=3)

3.3 Transmission Electron Microscopy

TEM measurement was used to study the morphology of NLC (Fig. 2). From Fig. 2, it can be seen that DTX-NLCs and blank-NLCs were spherical or elliptical in shape and were evenly distributed in the inner grid structures.^[18,23] The blank NLC and DTX-NLC had similar characters, which demonstrated that the entrapment of DTX would not significantly influence the shape of the NLC. DLS measurement of non-spherical particles will have deviation due to the assumption of the theoretical model of DLS is to test monodisperse and spherical particles. Non-spherical particles cause broadening of the particle size distribution as compared to the equivalent volume distribution. Moreover, the median and mean diameter may be shifted, often to a larger size. According to TEM images, the particle size of blank-NLC ranged from 95 nm to 180 nm, and the particle size of DTX-NLC ranged from 120 nm to 200 nm. These results are in agreement with the DLS results, where the particle size of blank-NLC and DTX-NLC were 136.4 ± 3.5 nm and 145.6 ± 2.5 nm, respectively.

Fig. 2. TEM image of blank NLC (A) and DTX-NLC (B)



3.4 Small Angle Neutron Scattering (SANS)

SANS was used to study the effects of DTX on structure changes of NLC (Fig 3A). Scattering data have been analyzed by dimensional analysis. The scattering intensity $I(q)$ can be described as $I(q) \sim q^{-\alpha}$. The exponent indicates that the microscopic structure on the 1-100 nm lengthscale, as seen by scattering, can be **understood** as fractals (mass or surface fractals) or strongly polydisperse nonfractal objects. Mass fractals mean open structures, whereas surface fractals describe dense materials with rough surfaces. The angular coefficient of the $\log I(q)$ versus $\log q$ plot is related to the dimensions of mass and surface fractal, D_v and D_s as $\alpha = 2 \times D_v - D_s$. If $1 < \alpha < 3$, the curve is associated with mass fractal. In our system, the surface and the bulk of the particles are not uniformly dense; thus the surface and the inner part of structure have the same fractal dimension ($D_v = D_s$). When $3 < \alpha < 4$, the materials have surface-fractal behavior with dense core ($D_v = 3$) and $D_s = 6 - \alpha$. The obtained value of α is equal to -3.33 for blank NLC, which corresponds to surface fractals structure of aggregates in solution. In the high q part of the scattering curve, α is equal to -4 (DTX-NLC), which corresponds to smooth surface of aggregates. **The loading of DTX into NLC can change the surface of NLC, which become smoother, and this result further confirmed that DTX was entrapped into NLC.**

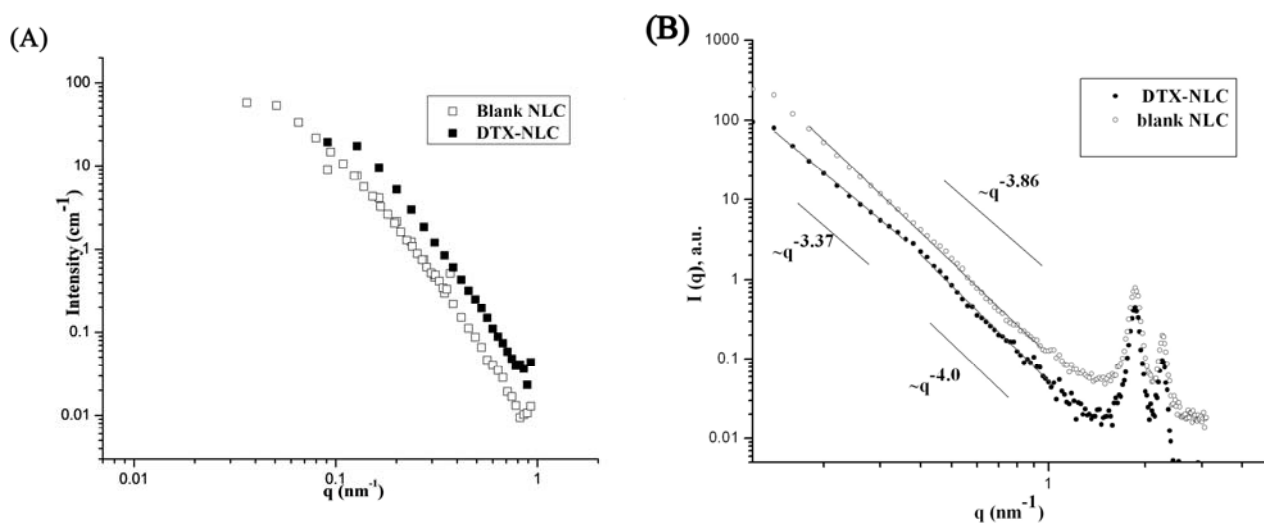
3.5 Small Angle X-Ray Scattering (SAXS)

The three-dimensional structures of freeze-dried DTX-NLC and blank NLC were studied by SAXS. There were two peaks (Fig. 3B, $q = 1.86 \text{ nm}^{-1}$, 2.26 nm^{-1} for DTX-NLC; $q = 1.86 \text{ nm}^{-1}$, 2.27 nm^{-1} for blank NLC), indicating that both DTX-NLC and

blank NLC arranged into cubic 3-dimensional structures. ^[48] Addition of DTX into NLC did not change the cubic structure of the blank NLC. The regular crystalline-like structure is expected to be good for sustained release profile. The solid matrix of NLC contains tiny liquid nanocompartments of oil. In these oil compartments the drug solubility is higher, thus increasing the total drug loading capacity. The nanocompartments are surrounded by solid lipid matrix, allowing prolonged drug release. ^[44] Also NLC is composed of solid lipid and liquid lipid, and such complex structure is beneficial for sustained drug release. ^[45]

The low q part of SAXS data has been analyzed by dimensional analysis similar to SANS data obtained for NLC samples. For blank NLC, the slope remained constant at 3.86 (in qualitative agreement with solution data) and indicated surface fractal. For DTX-NLC a crossover from slope of 3.37 (surface fractal) to 4 (smooth surface) at $q = 0.36 \text{ nm}^{-1}$ was observed. The large q part was similar to solution scattering data and the position of the crossover indicates the size of primary aggregates forming fractal cluster $\sim 2 \text{ nm}$.

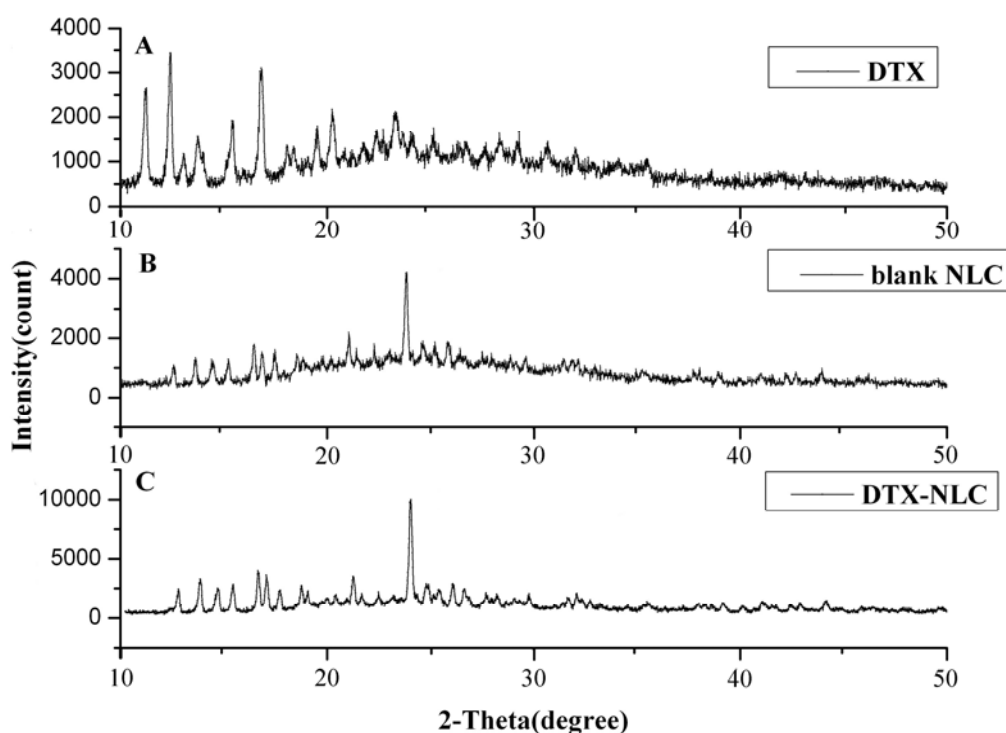
Fig.3. A: Effect of DTX on SANS spectra of NLC in PBS (pH 7.4); B: SAXS spectra of freeze-dried NLC with and without DTX



3.6 Wide angle X-ray powder diffraction(XRD)

Fig. 4. X-ray diffraction analysis of docetaxel formulations. X-ray powder diffractograms of DTX

(A), freeze-dried unloaded blank NLC (B) and freeze-dried DTX-NLC (C)



XRD was used to study the changes of microstructure in NLC and the state of DTX in NLC. XRD analysis made it possible to assess the length of the long and short spacing of the lipid lattice. In Fig.4, several characteristic diffraction peaks of pure DTX can be detected in 2θ scattered angle 11° , 13° , 14° , 16° and 17° . The blank NLC and DTX-NLC show one significant peak (24°). Consequently, the crystallites of pure DTX disappeared after being loaded in NLC; we can assume that DTX had been fully solubilized by the NLC. In addition, the diffraction intensity of

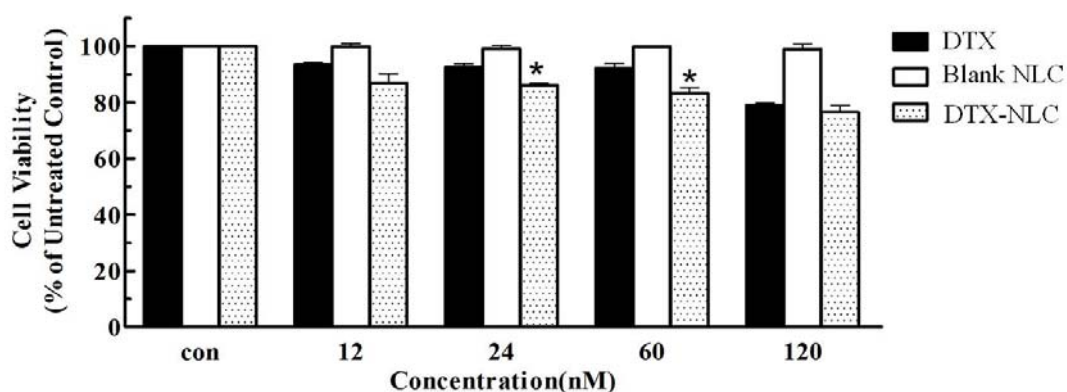
DTX-NLC was clearly stronger than that of blank NLC. This can be attributed to the less ordered microstructure of blank NLC in comparison to that of DTX-NLC. Thus the addition of DTX makes the DTX-NLC more crystalline.

3.7 *In vitro* cellular cytotoxicity assays (MTT)

In order to know the activity of DTX-NLC on cells, the cellular cytotoxicity was also evaluated by MTT assay. Fig. 5 revealed that in HeLa cells, DTX expressed significant cell growth inhibition effect as dose increasing. For example, the viability of HeLa cells treated with 24 nM DTX for 24 h was (92.4 ± 2.0) %, while 120 nM DTX treatments made the viability fall down to (78.9 ± 1.6) %. DTX-NLC possessed more inhibition potential than pure DTX at the concentration of 24 nM ($t = 4.85$, $P < 0.01$) and 60 nM ($t = 3.44$, $P < 0.05$) (Fig. 5). Also DTX-NLC showed higher cytotoxicity against HeLa cells at lower concentration than pure DTX at higher concentration. For example, the viability of HeLa cells treated with 12 nM DTX - NLC for 24 h was less than the one treated with 24 nM pure DTX for 24 h. However, at the concentration of 120 nM, both DTX and DTX-NLC exhibited significant but equivalent inhibition effects on HeLa cells. That is to say NLC slightly increased the treatment efficiency of relatively lower concentration of DTX, which might be due to the better solubility of DTX after being loaded into NLC. The more effective treatment of NLC formulations could be also attributed to the targeting ability of nanosized NLC, which were taken up into the cells more effectively. ^[49] In previous work, we performed the cell uptake studies in order to observe the intracellular distribution of NLC. ^[47] Those studies showed that NLC can rapidly enter into the

cell's cytoplasm, which can explain the slightly higher cytotoxicity of DTX/NLC compared to DTX alone. Small particles ranging between 120 and 200 nm only rarely undergo blood clearance by the cells of the reticulo-endothelial system (RES), therefore liver and spleen filtration is avoided, which means NLC has passive drug targeting property. [49] In addition, blank NLC showed <3% cytotoxicity.

Fig. 5. In vitro cytotoxicity of DTX and DTX-NLC against HeLa cells for 24 h. The cell viability was expressed as the percentage of untreated controls. Data were given as mean \pm SD (n=3). *p < 0.05 compared with DTX.



4. Conclusion

In this study, stable nanostructured lipid carrier with mean particle size less than 200 nm was successfully prepared by high-pressure homogenization. Docetaxel was used as active pharmaceutical ingredient to study the NLC effects on its drug effect. The mean particle size of DTX-NLC was in the range of about 120 nm to maximum 250 nm during the storage period of 30 days, with the entrapment efficiency decreasing from (60.5 \pm 5.0) % to (55.3 \pm 4.5) %. The microstructures of blank NLC and DTX-NLC were investigated by TEM, SANS and SAXS. The particles were spherical

or oval and had smooth surface, with a 3-dimensional cubic crystalline inner structure as revealed by TEM and SAXS. XRD results indicated that the adding of DTX to NLC made DTX-NLC more crystalline. The cytotoxicity was studied by MTT against HeLa cells. The data suggested that blank NLC was biocompatible with HeLa cells under test conditions and the carrier facilitated DTX to enter into cytosol and exhibited its antitumor effects. In this extent, NLC was helpful to decrease the volume of DTX but achieving the same therapy effects, while lower concentration of DTX was beneficial to normal tissue in clinical practice. However, DTX-NLC was ~~only~~ more effective than DTX **only at a** certain concentration, which was possibly related to the cell membrane permeability properties of DTX-NLC. The modification of NLC that makes the "carrier" more efficient and targets to the tumor cells is the issue should be further investigated. Overall performance of NLC **shows** significant potential and suggests that further investigations such as studying the relationship between microstructure of NLC and its release properties would be appropriate.

Acknowledgment

Aihua Zou gratefully acknowledges the support of this work by the Alexander von Humboldt Foundation. **Lihui Zhou is acknowledged for help during TEM measurements.** We gratefully acknowledge the support of this work by Chinese National Natural Science Foundation (201003047) and Fundamental Research Funds for the Central Universities. SANS measurements have been performed under support of the European Commission (Grant agreement N 283883-NMI3).

Reference

- [1] R.S. Mudshinge, A.B. Deore, S. Patil, C.M. Bhalgat, Nanoparticles Emerging carriers for drug delivery, Saudi Pharmaceutical Journal. 19 (2011) p.129
- [2] J.J. Wang, K.S. Liu, K.C. Sung, C.Y. Tsai, J.Y. Fang, Lipid nanoparticles with different oil/fatty ester ratios as carriers of buprenorphine and its prodrugs for injection, Eur. J. Pharm Sci. 38 (2009) p.138
- [3] M.D. Joshi, R.H. Müller, Lipid nanoparticles for parenteral delivery of actives, Eur. J. Pharm Biopharm. 71 (2009) p.161
- [4] D.M. Ridolfi, P.D. Marcato, G.Z. Justo, L. Cordi, D. Machado, N. Duran, Chitosan-solid lipid nanoparticles as carriers for topical delivery of tretinoin, Colloids, surf B: Biointerf. 93 (2010) p.36
- [5] S. Venkataraman, J.L. Hedrick, Z.Y. Ong, C. Yang, P.L.R. Ee, P.T. Hammond, Y.Y. Yang, The effects of polymeric nanostructure shape on drug delivery, Adv. Drug. Deliv. Rew. 63 (2011) p.1228
- [6] A.P. Nayak, W. Tiyaboonchai, S. Patankar, B. Madhusudhan, E.B. Souto, Curcuminoids-loaded lipid nanoparticles Novel approach towards malaria treatment, Colloids. Surf B: Biointerf. 81 (2010) p.263
- [7] C.R. Yang, X.L. Zhao, H.Y. Hu, K.X. Li, X. Sun, L. Li, D.W. Chen, Preparation, Optimization and Characteristic of Huperzine A Loaded Nanostructured Lipid Carriers, Chem. Pharm. Bull. 58 (2010) p.656
- [8] Y.C. Kuo, J.F. Chung, Physicochemical properties of nevirapine-loaded solid lipid nanoparticles and nanostructured lipid carriers, Colloids. Surf B: Biointerf. 83

(2011) p.299

[9] R.H. Müller, Lipid nanoparticles: recent advances, *Adv. Drug. Deliv. Rev.* 59 (2007) p.375

[10] J.E. Cortes, R. Pazdur, Docetacel, *J. Clin. Oncol.* 10 (1995) p.2643

[11] B. Chevallier, P. Fumoleau, P. Kerbrat, V. Dieras, H. Roche, I. Krakowski, N. Azli, M. Bayssas, M.A. Lentz, G.M. Van, Docetaxel is a major cytotoxic drug for the treatment of advanced breast cancer: a phase trial of the Clinical Screening Cooperative Group of European Organization for Research and Treatment of Cancer, *J. Clin. Oncol.* 2 (1995) p.314

[12] F.V. Fossella, J.S. Lee, D.M. Shin, M. Calayag, M. Huber, R. Perez-Soler, W.K. Murphy, S. Lippman, S. Benner, B. Glisson, Phase study of docetaxel for advanced or metastatic platinum-refractory non-small-cell lung cancer, *J. Clin. Oncol.* 3 (1995) p.645

[13] S.B. Kaye, M. Piccart, M. Aapro, P. Francis, J. Kavanagh, Phase trials of docetaxel (Taxotere) in advanced ovarian cancer an updated overview, *Eur. J. Cancer.* 13 (1997) p.2167

[14] W. Zhan, Y. Shi, Y. Chen, S. Yu, J. Hao, J. Luo, X. Sha, X. Fang, Enhanced antitumor efficiency by paclitaxel-loaded pluronic P123/F127 mixed micelles against non-small cell lung cancer based on passive tumor targeting and modulation of drug resistance, *Eur. J. Pharm. Biopharm.* 3 (2010) p.341

[15] H.J. Cho, H.Y. Yoon, H. Koo, S.H. Ko, J.S. Shim, J.H. Lee, K. Kim, I.C. Kwon, D.D. Kim, Self-assembled nanoparticles based on hyaluronic acid-ceramide (HA-

- CE) and Pluronic for tumor-targeted delivery of docetaxel, *Biomaterials*. 32 (2011) p.7181
- [16] I.V. Zhigaltsev, G. Winters, M. Srinivasulu, J. Crawford, M. Wong, L. Amankwa , D. Waterhouse, D. Masin, M. Webb, N. Harasym, L. Hrller, M.B. Bally, M.A. Ciufolini, P.R. Cullis, N. Maurer, Development of a weak-base docetaxel derivative that can be loaded into lipid nanoparticles, *J. Control. Release*. 144 (2010) p.332
- [17] Z.H. Xu, L.L Chen, W.W Gu, Y. Gao, L.P. Lin, Z.W. Zhang, Y. Xi, Y.P. Li, The performance of docetaxel-loaded solid lipid nanoparticles targeted to hepatocellular carcinoma, *Biomaterials*. 30 (2009) p.226
- [18] D.H. Liu, Z.H. Liu, L.L Wang, C. Zhang, N. Zhang, Nanostructured lipid carriers as novel carrier for parenteral delivery of docetaxel, *Colloid. Surf: B Biointerf*. 85 (2011) p.262
- [19] S. Naik, D. Patel, N. Surti, A. Misra, Preparation of PEGylated liposomes of docetaxel using supercritical fluid technology, *J. Supercrit. Fluid*. 54 (2010) p.110
- [20] X. Li, X. R. Li, X. Qian, Y. Ding, Y. Tu, R. Guo, Y. Hu, X. Jiang, B. Liu, Superior antitumor efficiency of cisplatin-loaded nanoparticles by intratumoral delivery with decreased tumor metabolism rate, *Eur. J. Pharm. Biopharm*. 70 (2008) p.726
- [21] H.Y. Hwang, I.S. Kim, I.C. Kwon, Y.H. Kim, Tumor targetability and antitumor effect of docetaxel-loaded hydrophobically modified glycol chitosan

nanoparticles, *J. Control. Release.* 128 (2008) p.23

- [22] A. Puri, E. Heldman, R. Blumenthal, **Lipid-Based Nanoparticles as Pharmaceutical Drug Carriers: From Concepts to Clinic**, *Crit. Rev. Ther. Drug Carrier Syst.* 26 (2009) p523
- [23] X. Li, D.K. Wang, Preparation and Pharmacokinetics of Docetaxel Based on Nanostructured Lipid Carriers, *J. Pharm. Pharmc.* 61 (2009) p.1485
- [24] X. Lin, R. Gao, X. Tang, Lipid Nanoparticles for Chemotherapeutic Applications: Strategies to Improve Anticancer Efficacy, *Exper Opin. Drug Deliv.* 9 (2012) p.767
- [25] C.Y. Zhuang, N. Li, M. Wang, X.N. Zhang, W.S. Pan, J.J. Peng, Y.S. Pan, T. Tang, Preparation and characterization of vinpocetine loaded nanostructured carriers (NLC) for improved oral bioavailability, *Int. J. Pharm.* 394 (2010) p.179
- [26] L. Rosta, Cold neutron research facility at the Budapest Neutron Centre, *Appl Phys. A.* 74 (2002) p.292
- [27] M. Gu, P. V. Suresh, Development, characterization and in vivo assessment of effective lipidic nanoparticles for dermal delivery of fluconazole against cutaneous candidiasis, *Chem.Phys.Lipids.* 165 (2012) p.454
- [28] B. Haley, E. Frenkel, Nanoparticles for drug delivery in cancer treatment, *Urologic Oncology Seminars and Original Investigations.* 26 (2008) p.57
- [29] S. Janos, M.M. Franco, R.A. Carl, **Complement Activation by Cremophor EL as a Possible Contributor to Hypersensitivity to Paclitaxel as In Vitro Study**, *J. NAT. Cancer I.* 90 (1998) p.300

- [30] M.P. Copper, M. Triesscheijn, I.B. Tan, M.C. Ruevekamp, F.A. Stewart, Photodynamic therapy in the treatment of multiple primary tumors in the head and neck, located to the oral cavity and oropharynx, *Clin Otolaryngol.* 32 (2007) p.185
- [31] H. Gelderblom, J. Verweij, K. Nooter, A. Sparreboom, Cremophor EL: the drawbacks and advantages of vehicle selection for drug formulation, *Eur. J. Cancer.* 37 (2001) p.1590
- [32] O. Carsten O, K. Oliver K, R.H. Müller, Lipase degradation of Dynasan 114 and 116 solid lipid nanoparticles (SLN)-effect of surfactants, storage and crystallinity, *Int. J. Pharm.* 237 (2002) p.119
- [33] S. Carsten, R.R. Barbara, G.K. Wolfgang, The influence of pulmonary surfactant on nanoparticulate drug delivery systems, *Eur. J. Pharm. Biopharm.* 77 (2010) p.350
- [34] A.A. Date, N. Vador, A. Jagtap, M.S. Nagarsenker, Lipid nanocarriers (Gelupearl) containing amphiphilic lipid Gelucire 50/13 as a novel stabilizer: fabrication, characterization and evaluation for oral drug delivery, *Nanotechnology.* 22 (2011) p.275120.
- [35] J.Y. Fang, C.L. Fang, C.H. Liu, Y.H. Su, Lipid nanoparticles as vehicles for topical psoralen delivery: solid lipid nanoparticles (SLN) versus nanostructured lipid carriers (NLC), *Eur. J. Pharm. Biopharm.* 70 (2008) p.633
- [36] C. Puglia, P. Blasi, L. Rizza, A. Schoubben, F. Rossi, M. Ricci, Lipid nanoparticles for prolonged topical delivery: an in vitro and vivo investigation,

Int. J. Pharm. 357 (2008) p.295

[37] A. Kovacevic, S. Savic, G. Vuleta, R.H. Müller, C.M. Keck, Polyhydroxy surfactants for the formulation of lipid nanoparticles (SLN and NLC) Effects on size, physical stability and particle matrix structure, Int. J. Pharm. 406 (2011) p.163

[38] S. Patricia, C.P. Samatha, Polymorphism, Crystallinity and Hydrophilic Lipophilic Balance of Stearic Acid and Stearic Acid-Capric/Caprylic Triglyceride Matrices for Production of Stable Nanoparticles, Colloids. Surf B: Biointerf. 86 (2011) p.125

[39] T. Radheshyam, P. Kamla, Nanostructured Lipid Carrier Versus Solid Lipid Nanoparticles of Simvastatin: Comparative Analysis of Characteristics Pharmacokinetics and Tissues Uptake, Int. J. Pharm. 415 (2011) p.232

[40] W Mehnert, K Mäder, Solid lipid nanoparticles: production, characterization and applications, Drug. Deliv. Rev. 47 (2001) p.165

[41] J.A. Champion, S. Mitragotri, Role of target geometry in phagocytosis, Proc. Natl, Acad. Sci. USA. 103 (2006) p.4930

[42] K. Zheng, A.H. Zou, The effect of polymer-surfactant emulsifying agent on the formation and stability of α -lipoic acid loaded nanostructured lipid carriers (NLC), Food Hydrocolloids. 32 (2013) p.72

[43] R.H. Müller, S. Gohla, Solid lipid nanoparticles (SLN) for controlled drug delivery a review of the state of the art, Eur. J. Pharm. Biopharm. 50 (2000) p.161

- [44] R.H. Müller, M. Radtke, Nanostructured Lipid Matrices for Improved Microencapsulation of Drugs, *Int. J. Pharm.* 242 (2002) p.121
- [45] R.H. Müller, S.A. Wissing, Solid lipid nanoparticles (SLN) and nanostructured lipid carriers (NLC) in cosmetic and dermatological preparation, *Drug. Deliv. Rev.* 54 (2002) p.131
- [46] A.Z. Mühlen, C. Schwarz, Solid lipid nanoparticles (SLN) for controlled drug delivery – Drug release and release mechanism. *Eur. J. Pharm. Biopharm.* 45 (1998) p.149
- [47] X.M. Yang, A.H. Zou, Preparation and Characterization of 4-dedimethylamino sancycline (CMT-3) Loaded Nanostructured Lipid Carrier (CMT-3/NLC) Formulations, *Int. J. Pharm.* 450 (2013) p.225
- [48] K. Brandenburg, W. Richter, M.H.J. Koch, H.W. Meyer, U. Seydel, Characterization of the nonlamellar cubic and H II structures of lipid A from *Salmonella enterica* serovar Minnesota by X-ray diffraction and freeze-fracture electron microscopy, *Chem.Phys.Lipids.* 91 (1998) p.53
- [49] E.B. Souto, R.H. Müller, Lipid Nanoparticles Effect on Bioavailability and Pharamcokinetic Changes, *Drug Deliv.* 197 (2011) p.115

Table Figures:

Table 1 The surface tension of F68/EL aqueous solutions at different molar ratio and concentration. Values are mean \pm SD (n=3). Page 11

Table 2 The mass ratio between different lipids ingredients. Page 12

Table 3 Physical characterization of blank and DTX-NLC in day 1 and day 30 after preparation. Page 14

Figure Legends:

Fig. 1. The mean particle size and polydispersity index of DTX-NLC with different lipids ingredients in the storage of 8 days. Page 12

Fig. 2. The TEM photograph of blank NLC (A) and DTX-NLC (B). Page 15

Fig. 3. A: Effect of DTX on SANS spectra of NLC in PBS (pH 7.4); B: SAXS spectra of freeze-dried NLC with and without DTX. Page 16

Fig. 4. X-ray diffraction analysis of docetaxel formulations. X-ray powder diffractograms of DTX (A), freeze-dried unloaded blank NLC (B) and freeze-dried DTX-NLC (C). Page 16

Fig. 5. In vitro cytotoxicity of DTX and DTX-NLC against HeLa cells for 24 h. The cell viability was expressed as the percentage of untreated controls. Data were given as mean \pm SD (n=3). *p < 0.05 compared with DTX. Page 18